Activity in primary visual cortex predicts performance in a visual detection task

David Ress, Benjamin T. Backus and David J. Heeger

Stanford University, Dept. of Psychology, 450 Serra Mall, Bldg. 420/400, Stanford, California 94305-2130, USA
Correspondence should be addressed to D.J.H. (heeger@stanford.edu)

Visual attention can affect both neural activity and behavior in humans. To quantify possible links between the two, we measured activity in early visual cortex (V1, V2 and V3) during a challenging pattern-detection task. Activity was dominated by a large response that was independent of the presence or absence of the stimulus pattern. The measured activity quantitatively predicted the subject's pattern-detection performance: when activity was greater, the subject was more likely to correctly discern the presence or absence of the pattern. This stimulus-independent activity had several characteristics of visual attention, suggesting that attentional mechanisms modulate activity in early visual cortex, and that this attention-related activity strongly influences performance.

Our ability to perform visual discrimination tasks is improved when we are instructed in advance when and where to attend to a visual stimulus[1–3]. Neuronal activity in several areas of visual cortex, including primary visual cortex (V1), can be modified by attention[4–20]. For example, in macaque monkeys, stimulus-evoked electrophysiological responses in extrastriate areas are enhanced by attention[4,11–14], and similar results are observed in human subjects with neuroimaging[6–10]. These neuronal correlates of attention are spatially selective[7–10] and depend on task difficulty[20]. Most notably, baseline firing rates in monkey extrastriate visual cortex are elevated by attention even without visual stimulation[13], and analogous phenomena are observed in humans[5,6,10]. It has not yet been determined, however, if the attention-related increase in baseline activity reported in these studies is actually relevant to behavior.

The main goal of the experiments reported here was to establish a relationship between V1 activity and behavioral performance. Event-related functional magnetic resonance imaging (fMRI)[21–24] was used to measure cortical activity while subjects performed a challenging pattern-detection task at contrast threshold. We observed a large, stimulus-independent response in V1, V2 and V3, which we call the base response. We infer that this base response corresponds to an increase in the baseline firing rates of a large number of neurons. Remarkably, the trial-to-trial variability in the base response in all these areas predicted behavioral performance on the task; performance was best (more correct judgments, largest d') when the base response was large and worst when the base response was small.

Results

Subjects viewed a uniform gray field and continuously fixated a small, high-contrast mark at its center (Fig. 1a and b) while lying in the bore of the magnetic resonance scanner. Once every 20 seconds, a short auditory tone cued subjects that a new trial was beginning. On half the trials (randomly interleaved), a low-contrast pattern was presented briefly in a peripheral annulus around the fixation mark; on the other trials, no pattern was presented, and the display remained gray. Subjects pressed one of two buttons to indicate whether they believed the pattern was present. Before commencing fMRI scanning sessions, subjects practiced the task extensively until their performance stabilized; this involved at least a dozen half-hour sessions over a three-week period. The contrasts used during the fMRI experiments were individually chosen so that each subject would perform with an accuracy of ~75% correct (d' ~1). The fMRI data were collected during several hundred trials for each of three subjects. Trials were categorized according to whether the stimulus pattern was present or absent, and whether the subject responded correctly or incorrectly. The fMRI data were analyzed separately for each of these four trial types.

Cortical activity in V1 was dominated by a large, stimulus-independent base response (Fig. 1c). This response was very similar for pattern-present (filled symbols) and pattern-absent (open symbols) trials. The base response was readily evident and highly significant ($p \approx 0$) in all three subjects (Z-scores, DJH, 41.3; BTB, 16.1; DBR, 38.6). Based on the current understanding of fMRI signals[25–27], we infer that the underlying neuronal activity associated with the base response was largely confined to the first one or two seconds of each trial, and that the slow time course of the fMRI measurements reflects a sluggish change in local cerebral blood flow and oxygenation. We hypothesize that the base response reflects an attention-related increase in the baseline firing rates of a large number of visual cortex neurons.

Under the hypothesis that the base response reflects attentional mechanisms, one would expect it to be correlated with performance in the threshold detection task; performance should be best when the attention-related base response is large and worst when the base response is small. Indeed, the base response was highly predictive of behavioral performance (Fig. 2). The linear regression showed a statistically significant positive slope ($r = 0.90$; $p = 0.005$). This result was robust with respect to the binning of the data (Methods); the regression was statistically

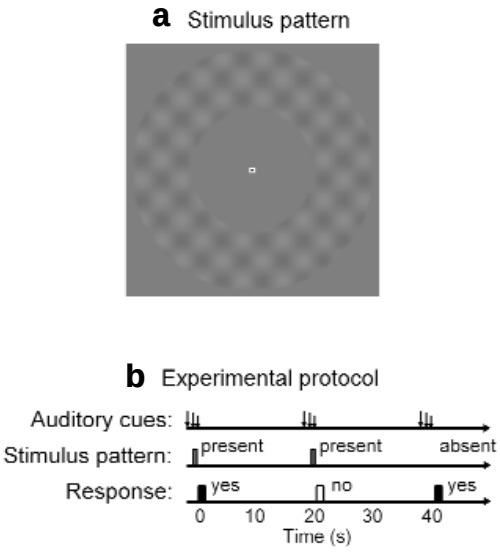

Fig. 1. Experimental protocol and typical result. (**a**) Subjects viewed a uniform gray field (27.3 cd/m2) while fixating a small, high-contrast mark. On each trial, either the display remained blank or a plaid pattern was presented briefly. The pattern, when present, was the sum of two sinusoidal gratings (0.5 cycles/degree), contrast-reversing (4 Hz), and confined to an annulus (3–6° radius). In the threshold detection experiments, the pattern was presented at contrasts of 0.8–0.9%, much lower than illustrated. (**b**) Trials began with an auditory warning tone. An auditory click at 1 s marked the onset of the stimulus period, which had a duration of 0.75 s. Another click (0.1 s later) signaled subjects to respond "yes" or "no" by pressing one of two buttons. Subjects then waited quietly for the next trial while maintaining fixation. No (correct/incorrect) feedback was provided to the subject. (**c**) V1 responses were large both for pattern-present (filled symbols) and pattern-absent (open symbols) trials. Each curve represents the average time course of the fMRI signal, averaged across many trials (163 pattern-present trials and 133 pattern-absent trials) and averaged throughout the region of cortical gray matter corresponding to the V1 representation of the stimulus annulus. Error bar indicates standard error at one time; other time points have similar standard errors.

significant ($p < 0.05$) for 5–25 bins. This result does not derive from individual differences between the subjects; the range of d′ values and the range of relative response amplitudes were similar in all three subjects.

The contingency between V1 activity and behavioral performance can be tested more rigorously by a logistic regression. We fit a logistic function to the subjects' performance on each trial as a function of the relative fMRI response amplitude on that trial (Methods). The slope of the best-fitting logistic function measures the strength of the predictive effect. For all subjects combined, the logistic regression was statistically significant, that is, the best-fit slope was reliably greater than zero ($p = 0.002$). The logistic regression was also statistically significant in two of three individual subjects (DJH, $p = 0.026$; BTB, $p = 0.060$; DBR, $p = 0.013$).

A third way to examine the relationship between V1 activity and behavior is to compare the base responses corresponding to correct and incorrect trials. For all subjects combined, the relative response amplitudes were larger for correct trials than for incorrect trials ($p = 0.002$). This difference was also statistically significant in two of three individual subjects (DJH, $p = 0.014$; BTB, $p = 0.052$; DBR, $p = 0.018$).

A stimulus-independent base response was also evident in extrastriate visual areas V2 and V3 (Fig. 3a and b). The responses in these areas were similar in shape and amplitude to those observed in area V1 (compare with Fig. 1c). We used the slope parameter of the logistic regression to quantitatively compare the three visual areas using data combined across all subjects (Fig. 3c). The base responses were predictive of behavioral performance in both extrastriate areas (V2, $p = 0.007$; V3, $p < 0.001$). The downward trend from V1 through V3 was not statistically significant. Individual subjects also showed significant effects in extrastriate areas (DJH, V2; BTB, V3; DBR, V2, V3).

Our interpretation of the contingency between cortical activity and behavioral performance relies on the hypothesis that the base response reflects attentional mechanisms. Indeed, the base response exhibited two critical characteristics of visual attention: it was spatially selective, and it depended on task difficulty. The base response was smaller in the subregions of V1 corresponding to the central visual field and the far periphery than in subregions corresponding to the stimulus annulus (Fig. 4). A similar but weaker pattern of spatial selectivity was also evident in V2 and V3 (Fig. 5). Although the base response was evident in several of the retinotopically organized visual areas, it was essentially absent in a lateral region of the occipital lobe that is adjacent to these visual areas (data not shown). Hence, the base response was not an artifact of increased respiration or pulse during task performance, nor was it due to nonspecific arousal.

The base response depended on task difficulty, with activity decreasing as the task was made easier. In a separate series of experiments, we measured V1 activity while subjects performed comparatively easier tasks, detecting patterns with higher contrasts (Fig. 6). Subjects were instructed to perform the task as accurately as possible, but without exerting attention unneces-

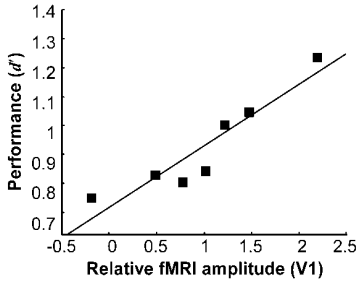

Fig. 2. Trial-to-trial variability in V1 activity was highly predictive of behavioral performance in the threshold detection task. Performance, as measured by d′, is highly correlated with the amplitude of V1 activity ($r = 0.92$; $p < 0.001$). Solid line is the linear regression.

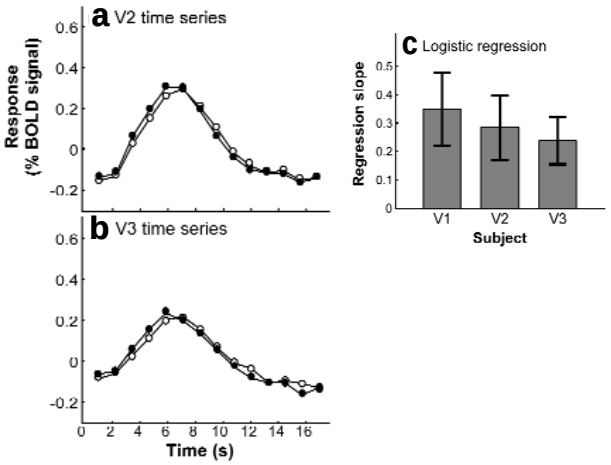

Fig. 3. Activity in extrastriate areas V2 and V3 predicted performance. (**a**, **b**) Typical time series (subject DBR) of activity in areas V2 and V3. Standard errors are similar to the size of the plot symbols. The amplitudes of the fMRI responses and the standard errors were similar to those in V1 (compare with **Fig. 1c**). (**c**) Slope of the best-fitting logistic function for each of the three visual areas. All three visual areas showed a reliable contingency between cortical activity and behavioral performance.

sarily. At higher contrasts, performance was 100% correct, and the base responses were small. The absolute amplitudes of the pattern-absent V1 responses were considerably smaller at 50% contrast (Fig. 6e) than at contrast threshold (Fig. 6a); this difference in V1 activity was statistically significant for each of the three subjects individually ($p < 0.001$, ~5:1 geometric mean ratio across the three subjects). A similar dependence on task difficulty was also observed for the base responses in areas V2 and V3 (Fig. 7). The stimulus-evoked increment in the pattern-present responses increased with stimulus contrast (Figs. 6 and 7), consistent with previous measurements of activity in human and monkey visual cortex[27–31].

Discussion

Our results lead us to hypothesize that attention, cortical activity and behavioral performance are linked. The base response probably reflects the activity of attentional mechanisms. This hypothesis is supported by the dependence on task difficulty and by the spatial selectivity of the base response, two defining characteristics of visual attention. In macaque monkeys, attention can cause an increase in the baseline firing rates of neurons in V2 and V4 (ref. 13), secondary visual areas that receive projections from V1. We suggest, therefore, that the base response that we observed reflects a small increase in the baseline firing rates of a very large number of neurons whose receptive fields overlap the stimulus annulus. Increasing baseline firing rates may potentiate an enhancement in the stimulus-evoked responses, which could improve the signal-to-noise ratio in the sensory representation of the stimulus by biasing neurons into a more sensitive segment of their operating range[12]. We attribute the contingency between V1 activity and performance to trial-to-trial fluctuations in attention (for example, lapses in attention or spatial uncertainty). We suggest that variability in the observers' attentional state causes variability in the baseline firing rates, which, in turn, causes variability in performance.

The pattern-present response increments evident at higher contrasts (Fig. 6), on the other hand, probably reflect the stimulus-evoked activity in the minority of neurons that are selective for the pattern. When the task is difficult and the sensory input small, measured cortical activity is dominated by small responses in each of a large number of neurons. When the task is easy and the sensory input large, measured cortical activity is dominated by large responses in each of a small number of neurons.

Activity in areas V1, V2 and V3 were all observed to predict behavioral performance, suggesting that these visual areas perform computations that are relevant to the contrast-detection task. We cannot distinguish whether the extrastriate base response was inherited from their V1 afferents, or if the V1 base response was caused by feedback from extrastriate cortex, or perhaps both.

Our main result, the contingency between attention-related cortical activity and behavioral performance, has been hinted at previously. Parietal lobe activity is correlated with performance (activity on correct-response trials greater than activity on incorrect-response trials) during a motion-detection task[32], although this result was not analyzed for statistical significance. It is possible that the attention-related signals that we have observed in early visual cortex derive from attentional control mechanisms in the parietal lobe, but our slice prescription did not allow us to examine such activity.

Eye movements pose a potential confound for interpretation of our results, but it is likely that subjects maintained steady fixation while performing the detection task. If subjects had moved their eyes, the shift of the fixation mark would have evoked activity in the foveal representation of V1; we see relatively little activity in this region (Figs. 4 and 5). Second, in control experiments, performance was not improved by allowing subjects to break fixation; best performance was obtained when the eyes were held steady on the fixation mark.

The interpretation of fMRI data depends on the sequence of events from the neuronal response to the fMRI signal, which is only partially understood[25,26]. For example, the fMRI signal might reflect not only neuronal firing rates but also subthreshold synaptic activity (due to simultaneous excitation and inhibition), which would be invisible to the extracellular electrode. However, the available data suggest that the fMRI signal is

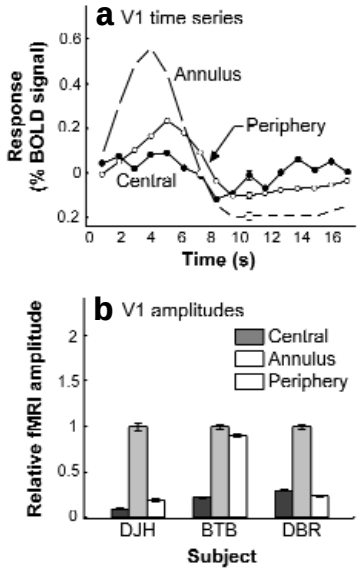

Fig. 4. V1 activity was spatially selective. A larger response was observed in regions corresponding to the stimulus annulus than in regions corresponding to the fovea or the periphery. (**a**) Sample fMRI time series (subject DJH). (**b**) Relative fMRI response amplitudes for all subjects.

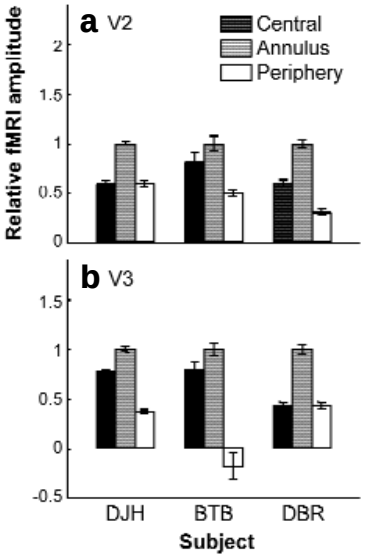

Fig. 5. Extrastriate activity was also spatially selective. (**a**) V2; (**b**) V3.

roughly proportional to average firing rates[33–37], even under conditions that seem to involve synaptic inhibition[33]. Moreover, the strong correlation that we observed between our brain and behavior measurements is striking: the fMRI signal is measuring what seems to be behaviorally relevant cortical activity.

Many electrophysiological studies report that baseline firing rates do not increase with attention (for example, ref. 14). Moreover, the studies that do find baseline increases in extrastriate cortex fail to find them in V1 (for example, ref 13). There are at least six possible explanations for the discrepancy between those results and our results (along with ref. 10), which do indicate baseline increases in V1. First, because cortical neurons generally have low baseline firing rates, the responses of many neurons must be recorded to obtain statistically significant results. Therefore, these effects may be better revealed by fMRI measurements, which reflect the activity of a large population of neurons. Second, as mentioned above, the fMRI measurement may reflect subthreshold activity that would be invisible to extracellular electrodes. Third, our data suggest that reliable and robust increases in baseline firing rates may be evident only when performing a particularly demanding task. The studies that failed to find baseline increases may have been using tasks that did not place sufficiently high demands on spatial attention. Fourth, the monkeys in those experiments may have been so highly trained that the usual attentional mechanisms were no longer needed to perform the task; training can have a critical effect on attentional signals[38]. Fifth, small shifts in eye position, equal in size to the V1 receptive fields, present a difficulty for the electrophysiology experiments. If eye position is systematically correlated with shifts in spatial attention, then the responses of individual V1 neurons will modulate as the receptive fields are shifted toward and away from the stimulus. These biases can be avoided by carefully accounting for eye position[14], but perhaps at the cost of underestimating the magnitude of the attentional effects. Small shifts in eye position do not present a difficulty in the fMRI experiments because they have a negligible effect on measurements of pooled neuronal activity. Sixth, there may be a genuine species difference.

We conclude that during threshold pattern detection, when sensory input is small and attentional demands are large, activity in early visual cortex is dominated by a stimulus-independent response that seems to be related to visual attention. This activity is strongly correlated with behavioral performance. Our results suggest that attention-related activity in primary visual cortex affects performance accuracy during a visual task.

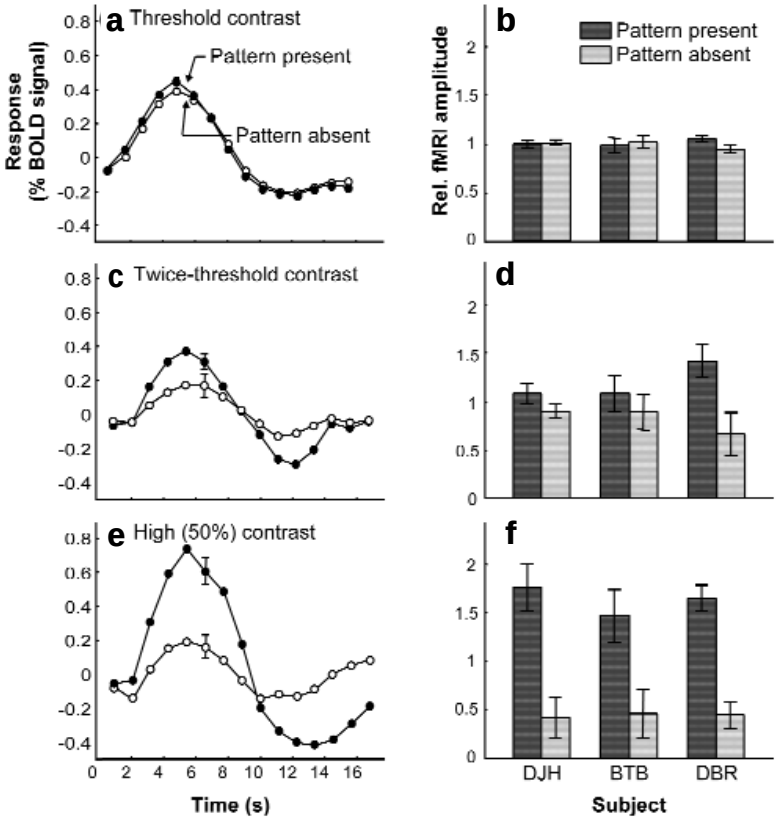

Fig. 6. V1 activity depended on task difficulty. (**a**) Typical fMRI time series for threshold-contrast stimuli (same as **Fig. 1c**, subject DBR). (**b**) Relative fMRI response amplitudes for threshold-contrast stimuli. Error bars represent 1 standard error (subject DBR, 0.85% stimulus contrast, n = 656 trials; DJH, 0.9% contrast, n = 456; BTB, 0.85% contrast, n = 400). (**c**) Example fMRI time series (subject DBR) for roughly twice the threshold stimulus contrast, so that performance was 100% correct. The base response was smaller than that measured at threshold (compare open symbols with those in **a**). (**d**) For contrasts roughly twice threshold, the pattern-present responses were larger than the pattern-absent responses, although this was statistically significant in only one subject (DBR, stimulus contrast, 2%, n = 36 trials, $p < 0.01$; DJH, 1.5% contrast, n = 96, $p = 0.07$; BTB, 2% contrast, n = 36, $p = 0.23$; one-tailed t-tests). (**e**) Example fMRI time series (subject DBR) for 50% stimulus contrast. (**f**) At high contrast, the base responses were small for all three subjects, and the pattern-present responses were much larger than the pattern-absent responses ($p < 0.001$ for each subject).

METHODS

Magnetic resonance (MR) imaging was done on a standard clinical GE 1.5 Tesla Signa scanner with a custom designed dual surface coil. The experiments were undertaken with the written consent of each subject, and in compliance with the safety guidelines for MR research. Each subject participated in several MR scanning sessions: one to obtain a high-resolution anatomical volume; one to functionally define the early, retinotopic visual areas, including V1, V2 and V3; one to functionally define the subregions of these visual areas that correspond to the stimulus annulus, and several sessions (9 for DBR, 6 for DJH and 6 for BTB) to measure fMRI responses in the various experimental conditions. For each subject, at least four sessions were specifically devoted to the threshold-detection task, whereas two sessions were devoted to examining the effects of higher-contrast stimuli. In these latter sessions, four-minute scanning blocks of higher-contrast stimuli were interleaved with blocks of threshold-contrast stimuli.

Stimuli were presented on a flat-panel display (NEC, multisynch LCD 2000) placed within a Faraday box with a conducting glass front, positioned near the subjects' feet. Subjects lay on their backs in the bore of the MR scanner and viewed the display through binoculars with a pair of angled mirrors attached just beyond the two objective lenses. Each subject had normal or corrected-to-normal vision.

Each MR scanning session began with the acquisition of a set of anatomical images using a T1-weighted fast spin-echo pulse sequence in the same slices as the functional images (TR = 500 ms, TE = 15 ms, echo-train length of 2, FOV = 240 mm, 4-mm slice thickness). The eight slices were arranged obliquely, perpendicular to the calcarine sulcus, with the most caudal slice approximately tangential to the occipital pole

These in-plane anatomical images were aligned to a high-resolution anatomical volume (acquired using a three-dimensional SPGR pulse sequence and a head coil) of each subject's brain so that all MR images (across multiple scanning sessions) from a given subject were coregistered. The alignment was done using an intensity-based algorithm that was specifically designed to deal with the variable contrast and intensity profiles produced by the different pulse sequences and different coils, to an accuracy of ~1 mm (ref. 39). The alignment algorithm computed a rigid-body coordinate transformation that maps the coordinates of each in-plane voxel to the corresponding coordinates in the high-resolution anatomical volume. Given this coordinate transformation, we used a standard image resampling technique (backward mapping with nearest-neighbor, point sampling) to transform the functional imaging data from the in-plane images to the volume. The end result was a time-series of data for each gray matter voxel from each fMRI scan.

The fMRI data were analyzed in each of three regions of interest (ROIs) corresponding to the V1, V2 and V3 representations of the stimulus annulus. These ROIs were defined, separately for each subject, in two steps. First, the retinotopically organized visual areas were identified, following well-established methods[40–43], by measuring the polar angle component of the cortical retinotopic map. Second, subregions of these visual areas that corresponded to the cortical representation of the stimulus annulus were further delimited based on a separate series of fMRI measurements. During these scans, subjects held fixation while the display alternated every 20 s between a contrast-reversing, high-contrast, plaid pattern within the 3–6° radius annulus, surrounded by a uniform (luminance-matched) gray field, and its geometric complement, a flickering plaid pattern everywhere except the annulus. Data were averaged across 6–8 repeated scans, each with 6 cycles of alternation between the two stimulus conditions. The final ROIs were then defined as those subregions of V1, V2 and V3 that were strongly correlated with the stimulus alternations (V1, $r > 0.7$; V2, $r > 0.5$; V3, $r > 0.4$; all regions, 0–10 s time lag).

Although we also defined additional retinotopic visual areas (V4v and V3a), the data were analyzed only in V1, V2 and V3 because V4v was too far anterior to be fully included in the slice prescription for all subjects, and noise levels were too high to reliably resolve the V3a representation of the stimulus annulus.

During each pattern-detection fMRI scan, subjects performed 12 consecutive trials (20- or 21-s duration) while a time series of volumes were acquired (every 1 or 1.5 s) using a T2*-sensitive, spiral-trajectory, gradient-echo pulse sequence[44,45]. For our particular scanner hardware, spiral fMRI pulse sequences compare favorably with echo-planar imaging in terms of sensitivity, and spatial and temporal sampling resolution (A.M. Sawyer-Glover & G.H. Glover, *SMRT Seventh Annual Meeting 69*, Sydney, 1998). Pulse sequence parameters for the fMRI scans were TE = 40 ms, TR = 500 (or 750) ms, FA = 55° (or 65°), FOV = 240 mm, effective in-plane pixel size of 3.2 × 3.2 mm, slice thickness of 4 mm. These pulse sequence parameters were chosen to optimize signal-to-noise ratio: the minimum number of slices to cover the desired brain regions, fast TR to acquire more temporal frames, and the largest voxel size that allowed for accurate and reliable localization of the retinotopic ROIs.

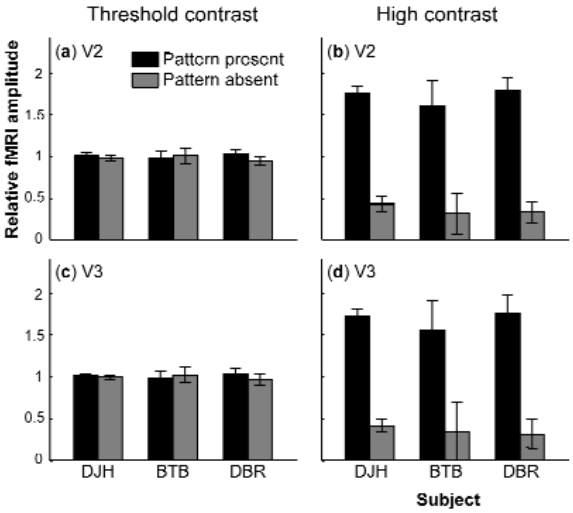

Fig. 7. Extrastriate activity also depended on task difficulty. (**a**, **b**) V2; (**c**, **d**) V3.

A bite bar stabilized the subjects' heads. The time series of fMRI images from each scan were visually inspected for head movements; 5 of approximately 260 total scans showed evidence of head movements and were excluded from further analysis.

Data from the first six seconds of each fMRI scan (before the first pattern-detection trial) were discarded to minimize transient effects of magnetic saturation. The fMRI time series were preprocessed by high-pass filtering them at each voxel to compensate for the slow signal drift we typically observe in our fMRI signals[46], and by dividing each voxel's time series by its mean intensity to convert the data from arbitrary image intensity units to percent signal modulation and to compensate for the decrease in mean image intensity with distance from the surface coil. The resulting time series were averaged throughout the region of cortical gray matter corresponding to the V1 representation of the stimulus annulus (and likewise for V2 and V3).

Relative fMRI response amplitudes were computed from these spatially averaged time series as follows. Regard each trial's time series as a vector, R*i*, where *i* is the trial index. All *N* trials of a particular fMRI scanning session were averaged together, as in Fig. 1c, but regardless of trial type, to create a session-mean time series,

$$\bar{\mathrm{R}} = \frac{1}{\mathrm{N}} \sum_{i+1}^{N} \mathrm{R}_i .$$

Next, we computed a normalized relative amplitude for each trial, A_i by projecting (inner product) the time series from each individual trial onto the session-mean time series and dividing by the squared norm of the session-mean time series:

$$A_i = \frac{\bar{\mathrm{R}}_i \bullet \mathrm{R}}{\|\bar{\mathrm{R}}\|^2} .$$

These calculations were done separately for each scanning session because of substantial session-to-session variations in the hemodynamic response[47]. Thus, we forced the average amplitude for all trials within a

session to be unity. Finally, we sorted the trials by type (pattern-present, pattern-absent) and computed the mean and standard error of the relative amplitudes across multiple scanning sessions.

Three schemes were used to test the contingency between behavioral performance and cortical activity. First, the relative fMRI response amplitudes, which fluctuated greatly from trial to trial, were sorted into ascending order, then divided into bins, each containing the same number of trials. Each trial within a bin is associated both with a relative fMRI response amplitude and with the task-related behavioral data (that is, whether the stimulus pattern was absent or present, and whether the subject's button press was correct or incorrect). For each bin, we computed the average fMRI amplitude, and we computed d′, a measure of the behavioral performance calculated from the percentage of hits, misses, false alarms and correct rejections[48]. In the second scheme, a logistic function was fit to the binary (correct/incorrect) performance data for all individual trials, as a function of the relative fMRI response amplitude. The form of the function was

$$P(A) = \frac{0.5 + \exp(a + bA)}{1 + \exp(a + bA)}$$

where A is the relative fMRI response amplitude for a given trial, $P(A)$ is the predicted probability that the subject was correct on that trial, and a and b are the parameters of the fit. The parameters a and b were adjusted by an optimization routine to match the measured probability of subjects' responses across all of the trials. The slope parameter, b, is a quantitative measure of the contingency between the fMRI amplitudes and the subjects' performance. The reliability of the estimate of b was determined using a statistical bootstrap procedure[49]. The third scheme was a straightforward comparison of the ensemble of relative response amplitudes corresponding to correct (hits, correct rejections) and erroneous (misses, false alarms) trials. We used a t-test on the hypothesis that the mean amplitude of correct trials was greater than the mean amplitude for erroneous trials.

Acknowledgements

We thank W.T. Newsome, B.A. Wandell and M. Carandini for comments. This research was supported by an NEI grant (R01-EY11794), a grant from the Human Frontier Science Program, and two NRSA postdoctoral research fellowships (F32-EY06899 and F32-EY06952).

Received 12 April; Accepted 10 July 2000

1. Pashler, H. E. *The Psychology of Attention* (MIT Press, Cambridge, Massachusetts, 1998).
2. Posner, M. I., Snyder, C. R. & Davidson, B. J. Attention and detection of signals. *J. Exp. Psychol.* 109, 160–174 (1980).
3. Graham, N. *Visual Pattern Analyzers* (Oxford Univ. Press, New York, 1989).
4. Desimone, R. & Duncan, J. Neural mechanisms of selective visual attention. *Annu. Rev. Neurosci.* 18, 193–222 (1995).
5. Martínez, A. *et al.* Involvement of striate and extrastriate visual cortical areas in spatial attention. *Nat. Neurosci.* 2, 364–369 (1999).
6. Chawla, D., Rees, G. & Friston, K. J. The physiological basis of attentional modulation in extrastriate visual areas. *Nat. Neurosci.* 2, 671–676 (1999).
7. Brefczynski, J. A. & DeYoe, E. A. A physiological correlate of the 'spotlight' of visual attention. *Nat. Neurosci.* 2, 370–374 (1999).
8. Tootell, R. B. *et al.* The retinotopy of visual spatial attention. *Neuron* 21, 1409–1422 (1998).
9. Gandhi, S. P., Heeger, D. J. & Boynton, G. M. Spatial attention affects brain activity in human primary visual cortex. *Proc. Natl. Acad. Sci. USA* 96, 3314–3319 (1999).
10. Kastner, S., Pinsk, M. A., De Weerd, P., Desimone, R. & Ungerleider, L. G. Increased activity in human visual cortex during directed attention in the absence of visual stimulation. *Neuron* 22, 751–761 (1999).
11. Hillyard, S. A., Vogel, E. K. & Luck, S. J. Sensory gain control (amplification) as a mechanism of selective attention: electrophysiological and neuroimaging evidence. *Phil. Trans. R. Soc. Lond. B Biol. Sci.* 353, 1257–1270 (1998).
12. Reynolds, J. H., Chelazzi, L. & Desimone, R. Competitive mechanisms subserve attention in macaque areas V2 and V4. *J. Neurosci.* 19, 1736–1753 (1999).
13. Luck, S. J., Chelazzi, L., Hillyard, S. A. & Desimone, R. Neural mechanisms of spatial selective attention in areas V1, V2, and V4 of macaque visual cortex. *J. Neurophysiol.* 77, 24–42 (1997).
14. McAdams, C. J. & Maunsell, J. H. Effects of attention on the reliability of individual neurons in monkey visual cortex. *Neuron* 23, 765–773 (1999).
15. Colby, C. L., Duhamel, J. R. & Goldberg, M. E. Visual, presaccadic, and cognitive activation of single neurons in monkey lateral intraparietal area. *J. Neurophysiol.* 76, 2841–2852 (1996).
16. Motter, B. C. Focal attention produces spatially selective processing in visual cortical areas V1, V2, and V4 in the presence of competing stimuli. *J. Neurophysiol.* 70, 909–919 (1993).
17. Roelfsema, P. R., Lamme, V. A. & Spekreijse, H. Object-based attention in the primary visual cortex of the macaque monkey. *Nature* 395, 376–381 (1998).
18. Haenny, P. E. & Schiller, P. H. State dependent activity in monkey visual cortex. I. Single cell activity in V1 and V4 on visual tasks. *Exp. Brain Res.* 69, 225–244 (1988).
19. Haenny, P. E., Maunsell, J. H. & Schiller, P. H. State dependent activity in monkey visual cortex. II. Retinal and extraretinal factors in V4. *Exp. Brain Res.* 69, 245–259 (1988).
20. Spitzer, H., Desimone, R. & Moran, J. Increased attention enhances both behavioral and neuronal performance. *Science* 240, 338–340 (1988).
21. Ogawa, S., Lee, T. M., Kay, A. R. & Tank, D. W. Brain magnetic resonance imaging with contrast dependent on blood oxygenation. *Proc. Natl. Acad. Sci. USA* 87, 9868–9872 (1990).
22. Kwong, K. K. *et al.* Dynamic magnetic resonance imaging of human brain activity during primary sensory stimulation. *Proc. Natl. Acad. Sci. USA* 89, 5675–5679 (1992).
23. Ogawa, S. *et al.* Intrinsic signal changes accompanying sensory stimulation: functional brain mapping with magnetic resonance imaging. *Proc. Natl. Acad. Sci. USA* 89, 5951–5955 (1992).
24. Belliveau, J. W. *et al.* Functional mapping of the human visual cortex by magnetic resonance imaging. *Science* 254, 716–719 (1991).
25. Malonek, D. & Grinvald, A. Interactions between electrical activity and cortical microcirculation revealed by imaging spectroscopy: implications for functional brain mapping. *Science* 272, 551–554 (1996).
26. Buxton, R. B., Wong, E. C. & Frank, L. R. Dynamics of blood flow and oxygenation changes during brain activation: the balloon model. *Magn. Reson. Med.* 39, 855–864 (1998).
27. Boynton, G. M., Engel, S. A., Glover, G. H. & Heeger, D. J. Linear systems analysis of functional magnetic resonance imaging in human V1. *J. Neurosci.* 16, 4207–4221 (1996).
28. Tootell, R. B. *et al.* Functional analysis of human MT and related visual cortical areas using magnetic resonance imaging. *J. Neurosci.* 15, 3215–3230 (1995).
29. Boynton, G.M., Demb, J. B., Glover, G. H. & Heeger, D. J. Neural basis of contrast discrimination. *Vision Res.* 39, 257–269 (1999).
30. Carandini, M., Heeger, D. J. & Movshon, J. A. Linearity and normalization in simple cells of the macaque primary visual cortex. *J. Neurosci.* 17, 8621–8644 (1997).
31. Demb, J., Boynton, G. M. & Heeger, D. J. Functional magnetic resonance imaging of early visual pathways in dyslexia. *J. Neurosci.* 17, 8621–8644 (1997).
32. Shulman, G. L. *et al.* Areas involved in encoding and applying directional expectations to moving objects. *J. Neurosci.* 19, 9480–9496 (1999).
33. Heeger, D. J., Boynton, G. M., Demb, J. B., Seidemann, E. & Newsome, W. T. Motion opponency in visual cortex. *J. Neurosci.* 19, 7162–7174 (1999).
34. Wandell, B. A. *et al.* Color signals in human motion-selective cortex. *Neuron* 24, 901–909 (1999).
35. Seidemann, E., Poirson, A. B., Wandell, B. A. & Newsome, W. T. Color signals in area MT of the macaque monkey. *Neuron* 24, 911–917 (1999).
36. Rees, G., Friston, K. & Koch, C. A direct quantitative relationship between the functional properties of human and macaque V5. *Nat. Neurosci.* 3, 716–723 (2000).
37. Heeger, D. J., Huk, A. C., Geisler, W. S. & Albrecht, D. G. Spikes versus BOLD: What does neuroimaging tell us about neuronal activity? *Nat. Neurosci.* 3, 631–633 (2000).
38. Ito, M. & Gilbert, C. D. Attention modulates contextual influences in the primary visual cortex of alert monkeys. *Neuron* 22, 593–604 (1999).
39. Nestares, O. & Heeger, D. J. Robust multiresolution alignment of MRI brain volumes. *Magn. Reson. Med.* 43, 705–715 (2000).
40. Engel, S. A. *et al.* fMRI of human visual cortex. *Nature* 369, 525 (1994).
41. Engel, S. A., Glover, G. H. & Wandell, B. A. Retinotopic organization in human visual cortex and the spatial precision of functional MRI. *Cereb. Cortex* 7, 181–192 (1997).
42. Sereno, M. I. *et al.* Borders of multiple visual areas in humans revealed by functional magnetic resonance imaging. *Science* 268, 889–893 (1995).
43. DeYoe, E. A. *et al.* Mapping striate and extrastriate visual areas in human cerebral cortex. *Proc. Natl. Acad. Sci. USA* 93, 2382–2386 (1996).
44. Glover, G. H. & Lai, S. Self-navigated spiral fMRI: interleaved versus single-shot. *Magn. Reson. Med.* 39, 361–368 (1998).
45. Glover, G. H. Simple analytic spiral K-space algorithm. *Magn. Reson. Med.* 42, 412–415 (1999).
46. Smith, A. M. *et al.* Investigation of low frequency drift in fMRI signal. *Neuroimage* 9, 526–533 (1999).
47. Aguirre, G. K., Zarahn, E. & D'Esposito, M. The variability of human, BOLD hemodynamic responses. *Neuroimage* 8, 360–369 (1998).
48. Green, D. M. & Swets, J. A. *Signal Detection Theory and Psychophysics* (Peninsula Publishing, Los Altos, California, 1988).
49. Efron, B. & Tibshirani, R. J. *An Introduction to the Bootstrap* (Chapman & Hall, New York, 1993).